Green Chemistry

Accepted Manuscript

ROYAL SOCIETY OF CHEMISTRY

www.rsc.org/greenchem

Green Chemistry

RSCPublishing

ARTICLE

When can ionic liquids be considered readily biodegradable? Biodegradation pathways of pyridinium, pyrrolidinium and ammonium-based ionic liquids

Cite this: DOI: 10.1039/xoxxoooooox

Received ooth January 2012,
Accepted ooth January 2012

DOI: 10.1039/xoxxoooooox

www.rsc.org/

Y. Deng,[a,b] I. Beadham,[c] M. Ghavre,[c] M. F. Costa Gomes,[b,a] N. Gathergood,[c,d*] P. Husson,[a,b] B. Légeret,[b,a] B. Quilty,[e] M. Sancelme[a,b] and P. Besse-Hoggan,[b,a]*

Ionic liquids have been the subject of intense interest over the past decade, due to their unique structures, which can be tuned to modify the physicochemical properties of the solvent. Nevertheless, industrial processes rarely involve ILs, partly because our understanding of their environmental impact and biodegradability is still in its infancy. Biodegradability criteria for chemical compounds have been defined by the OECD, according to standard protocols in which a chemical is exposed to microbes in an activated sludge over a period of 28 days. However, most reports into IL biodegradation have concentrated on ultimate biodegradability, and have neglected to identify metabolites along the biodegradative pathway. In fact, intermediate metabolites can be more toxic than the parent molecule and may have a completely different environmental profile. We have studied the antimicrobial activities and biodegradation kinetics of ten pyridinium, pyrrolidinium and ammonium-based ionic liquids incubated with either a pure strain of *Rhodococcus rhodochrous* ATCC 29672 or an activated sludge, and have also determined their degradation pathways using ^{1}H NMR and LC-MS, with accompanying control experiments under abiotic conditions. Several intermediary metabolites were identified and quantified. All the ILs (except a long-chain alkylpyridinium in C_6) proved to be "readily biodegradable" with the pure strain (80 - 100 % degradation) under the conditions of the test which was not the case with activated sludges; however in 3 cases over 10, the biodegradation resulted in an undesirable accumulation of metabolites.

Introduction

Ionic liquids have been at the forefront of new solvent technologies development over the past decade. The unique physicochemical properties of these frequently bulky and unsymmetrical, low-melting point salts can be further 'tuned' for specific applications by choosing the most suitable anion-cation combination or by synthesizing a task specific ionic liquid (TSIL).[1-4]

TSILs are chemically functionalized to actively participate in processes such as catalysis or CO_2 capture, or to exhibit modified physico-chemical properties.

The negligible vapour pressure of ILs also makes them attractive for industrial processes that respect both occupational health and the environment.[5-6] Nevertheless, although ILs have been referred to as 'green solvents', they are neither intrinsically non-toxic, or without environmental impact if disposed of irresponsibly or by accident. For example, studies have demonstrated the toxicity of a variety of ILs to bacteria and algae, as well as more complex organisms, with experimental[7-16] but also theoretical approaches, efforts being carried out for the development of mathematical models to allow the prediction of the aquatic toxicity of ILs.[17-20] It has recently been proposed that the antimicrobial properties of some ILs may in fact lead to medical applications.[21-22] Another factor of concern is the resistance of some of the most common IL cations (e.g. dialkylimidazolium), and fluorinated anions to biodegradability.[23-34] Several strategies have been devised to increase the biodegradability of ILs by modifying the chemical structure of either the cation (imidazolium, pyridinium, and ammonium classes) or the anion. In previous studies,[23-25,28,29] we have demonstrated that the presence of oxygen-substituted chains on the imidazolium ring can reduce the antimicrobial toxicity and increase the biodegradability of 1-alkyl-3-methylimidazolium ionic liquids, incorporating either bis(trifluoromethylsulfonyl)imide or octylsulfate anions.

In most of the studies published, the criteria to assess biodegradability are the results of OECD and ISO assays such as the modified Sturm test (OECD 301 B), CO_2 headspace test (ISO 14593), or closed bottle test (OECD 301 D).[35] These experiments measure either the CO_2 produced or O_2 consumed during incubation of the organic compound with a mixed microbial population in sludge from a wastewater treatment plant over a given time.[36-37] These respirometric tests are subject to several limitations: (i) the activated sludge sample taken as an inoculum can greatly vary in microbial diversity, depending on the wastewater treatment plant chosen, and even can vary when sourced from the same plant, according to the season or to variations in the plant influent;[38-40] (ii) microbial respiration may be affected by the presence of chemicals even if they are not transformed or changed due to a variation/adaptation of the microbial community during the test.[34] A 'blank' experiment can therefore not act as a satisfactory negative control or (iii) the results obtained for 'readily biodegradable' compounds, *i.e.* those for which the level of biodegradation exceeds 60% within 28 d, seldom reflect the true environmental impact. Indeed, except in the case of complete mineralization (and in fact also in this case), metabolism can lead to the formation of intermediate or final transformation products which are more toxic, more persistent and more hazardous than the starting material and this should be taken into account to achieve a realistic evaluation for the life cycle assessment. Even intermediate reactive metabolites can interact with the ecosystem and have negative impact on the environment. Moreover, these tests can lead to inconsistent conclusions. For example, Kumar *et al.*[41] have reported the complete disappearance of 1-butyl-3-methylimidazolium, BF_4^- after 15 d of incubation with a strain of *Pseudomonas putida* and have identified degradation compounds, even though this IL was found to be recalcitrant in Sturm and closed-bottle assays.[30] Detailed investigations, identifying the chemical structures of metabolites formed, as well as measurements of degradation kinetics are crucial in order to realistically evaluate the behaviour of ILs in the environment. The toxicity of metabolites should also be tested, and this holistic approach has been followed, when biodegradation by an activated sludge was monitored by NMR or GC-MS for different ILs, in conjunction with toxicological studies.[26,29,34,36-37,42-47] However, biodegradation by a mixed microbial community may involve synergy between numerous microbial strains. This can pose difficulties if the objective is to develop an industrial bioremediation process, for which the identification of individual microbes acting in sludge is a complex process.

Therefore, we first investigated a pure isolated strain, *Rhodococcus rhodochrous* ATCC 29672, which is known to degrade a wide range of xenobiotics[48-49] and even some ILs.[29,] Then, in order to compare a single strain with a microbial community, we tested an activated sludge and evaluated the biodegradability of several pyridinium, pyrrolidinium and ammonium ILs in terms of kinetics, metabolite formation and quantification. These ILs were carefully chosen to incorporate side chains containing either oxygenated functional groups (alcohol, ester), or conventional alkyl chains to compare their biodegradation. The anti-microbial activity of these ILs was also assessed using a qualitative (Agar diffusion test) and a quantitative (Minimum Inhibitory Concentrations) methods to gain a more representative overview of their environmental impact, based on the major degradation products identified by ^{1}H NMR and LC-MS.

Materials and Methods

Chemicals.

The structures and abbreviations of the ILs used in this study are listed in Fig. 1. $[C_3Py][Tf_2N]$, $[C_{1COOC2}Py][Tf_2N]$, $[C_{3OH}Py][Tf_2N]$, $[C_1mPyr][Tf_2N]$ and $[NH_{112OH}][Ac]$ were purchased from Iolitec (Germany) and their purity is stated as > 98%. $[N_{1112OCOCH3}][Tf_2N]$ was purchased from Solvionic (France) and its purity is stated as > 98%. $[C_6mPy][Tf_2N]$, $[C_4mPyr][Tf_2N]$, $[N_{1114}][Tf_2N]$ and $[N_{1132OH}][Tf_2N]$ were supplied by Queen's University of Belfast, UK and their purity was determined by ^{1}H NMR to be > 99%.

Biodegradation of ILs by *Rhodococcus rhodochrous* ATCC 29672

1 Incubation. *Rhodococcus rhodochrous* ATCC 29672 was grown in 100-mL portions of Trypcase-soy broth (bioMérieux, Marcy l'Etoile, France) in 500-mL Erlenmeyer flasks incubated at 27 °C and 200 rpm. The cells (300 mL of the culture medium) were harvested after 24 h of culture under sterile conditions and centrifuged at 8000 rpm for 15 min at 4°C. The bacterial pellet was first washed with a NaCl solution (8 g L^{-1}) and then with Volvic® mineral water to maintain a constant mineral composition. The resting cells ($5x10^9$ cells mL^{-1}) were incubated with 50 mL of the IL solution (1 mM) in 250 mL Erlenmeyer flasks at 27 °C under agitation (200 rpm). Negative controls without cells (abiotic samples) or without substrate were carried out under the same conditions. Each flask was weighed regularly to account for possible water losses due to evaporation and completed with water. During the seven-week incubation, samples (1 mL) were taken regularly and centrifuged at 12,000 rpm for 5 min. The supernatants were immediately frozen after the experiment, until NMR analysis. All the experiments were carried out in duplicate.

2 ^{1}H Nuclear Magnetic Resonance (NMR) analyses. The crude samples (540 µL) were supplemented with 60 µL of a 5 mM solution of tetradeuterated sodium trimethylsilylpropionate (TSP-d_4, Eurisotop, Saint-Aubin, France) in D_2O. D_2O was used for locking and shimming. TSP-d_4 constituted a reference for chemical shifts (0

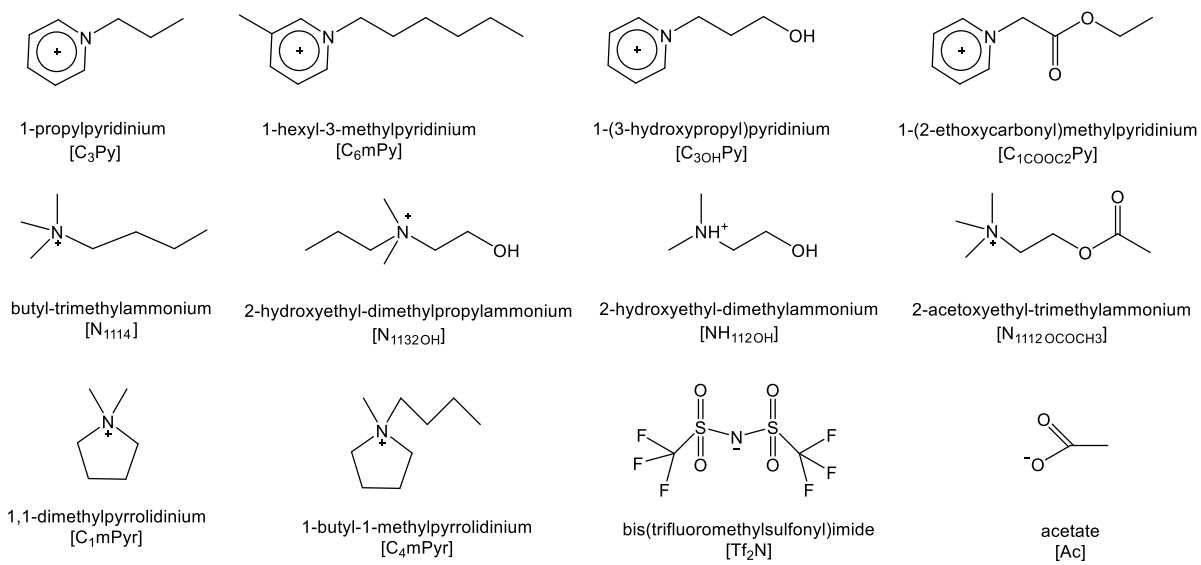

Fig. 1. Abbreviations, structures and names of the ions studied

ppm) and quantification. ^{1}H NMR was performed at 25 °C and 500 MHz on an Avance 500 Bruker spectrometer (Bruker Biospin, Wissembourg, France) equipped with a triple-resonance (^{1}H, ^{13}C, ^{15}N) inverse probe with 5-mm-diameter tubes containing 600 µL of sample, with water suppression by a classical two-phase shifted pulse saturation sequence. 128 scans were collected (90° pulse, 7.3 µs; saturation pulse, 3 s; relaxation delay, 3 s; acquisition time, 4.679 s; 65,536 data points). A 1-Hz exponential line-broadening filter was applied before Fourier transformation, and a baseline correction was performed on the spectra before integration using Bruker software (Topspin 2.0).

3 ^{19}F Nuclear Magnetic Resonance (NMR) analyses. ^{19}F NMR measurements were obtained using a Bruker Avance spectrometer at 376.49 MHz and 298 K with a 5-mm QNP ^{13}C/^{31}P/^{19}F-{^{1}H} probe equipped with a z-gradient coil. The ^{19}F 90° pulse length was 13.5 µs. The spectral width was 75,188 Hz. The number of data points used for acquisition was 131,072. Approximately 19,500 scans were recorded. A 1.5 s recycle delay was used. No ^{1}H decoupling was achieved.

4 LC-(+)-ESI-MS analyses. A Waters Alliance 2695/Micromass LC/Q-TOF (Micromass, Manchester, UK), equipped with an orthogonal geometry Z-spray ion source was used. The desolvation and ion source block temperatures were set at 300 °C and 120 °C, respectively. The source temperature allows the formation of a stable spray and minimizes droplets and water cluster formation. Gaseous N_2 was used as nebuliser gas (35 L h^{-1}) and desolvation gas (450 L h^{-1}). The optimum voltages found for the probe and ion source components (to produce maximum intensity) were 3 kV for the stainless-steel capillary, 3 5V for the sample cone and 1 V for the extractor cone. Before analysis, each sample was diluted by twenty and 10 µL were directly injected at 20 °C in the LC-MS system equipped with a photodiode array detector (DAD) (λ = 265 nm) without any further treatment, using the following HPLC conditions: HILIC phase column (Kinetex HILIC, Phenomenex, 2.6 µm, 100 mm × 2.1 mm) was used with a flow rate of 0.25 mL/min. For the gradient elution, solvent B buffer consisted of 95% acetonitrile and 5 mM ammonium formate buffer and solvent A 5% acetonitrile and 5 mM ammonium formate buffer. A linear gradient from 10% to 50% B in 8 minutes was employed and 40%B was kept until 15 min.

Activated sludge assay of biodegradation

1 Incubation. A preliminary primary biodegradation test was conducted using a modified OECD method (OECD 301A).[35] The inoculum used was an activated sludge (AS) mixed microbial community, issued from a pharmaceutical company's wastewater treatment facility (Dublin). The AS sample was washed to eliminate carryover of chemicals from the plant and then pre-conditioned by aeration at room temperature for 5 d. After aeration, the AS was washed three times with mineral nutrient medium.[35] The final supernatant was decanted and the solid sludge re-suspended in a mineral medium to give a concentration of 5 g L^{-1} suspended solids. The ILs [C_4mPyr][Tf_2N], [C_{3OH}Py][Tf_2N] and [N_{1132OH}][Tf_2N] were tested in duplicate at a concentration of 1 mM. All control flasks were also tested in duplicate. Sterile control flasks contain 1 mM IL and autoclaved inoculum. Positive control flasks containing reference standard sodium-*n*-dodecyl sulfate (SDS) (1 mM) and inoculated medium were also set up. Blank controls contained only inoculated mineral medium. Flasks containing the IL in the mineral medium as well as in distilled water in the absence of inoculum were prepared. All the test flasks were capped with cotton wool plugs and subsequently incubated at 100 rpm in the dark for 24 h. 1.5 mL samples were retrieved from the flasks immediately and at the 1st, 2nd, 4th, 7th, 10th, 14th and 21st day, and then centrifuged at 13,000 rpm for 6 min. The supernatants were immediately frozen, prior to final NMR analysis.

2 ^{1}H Nuclear Magnetic Resonance (NMR) analyses. The crude samples (570 µL) were supplemented with 30 µL of a 1% (w/vol) solution of tetradeuterated sodium trimethylsilylpropionate (TSP-d_4) in D_2O. ^{1}H NMR was performed on an Avance 600 Bruker spectrometer, with water suppression by a classical two-phase shifted pulse saturation sequence.

Anti-microbial activities

1 Adapted Agar diffusion test. The *in vitro* anti-microbial activity of the ILs was investigated against *Pseudomonas putida* strain CP1 and *Escherichia coli* DSMZ 498. The bacteria were incubated at 30 °C for 24 h. After incubation, cell suspensions were then spread uniformly onto agar plates and allowed to dry. Holes of 1.2 cm diameter were cut into the dry agar, and 50 µL aqueous solution of 2 g L^{-1} IL was introduced into the holes. Plates were incubated at 30 °C. The inhibition zone diameter was measured after 72 h of incubation.

2 Determination of the Minimum Inhibitory Concentration (MIC). Five strains were tested to assess the antimicrobial activity of the ILs: four bacteria (*Bacillus cereus* ATCC 14579 and *Rhodococcus rhodochrous* ATCC 29672 as Gram positive bacteria, *Pseudomonas aeruginosa* ATCC 17504 and *Escherichia coli* ATCC 11303 as Gram negative ones) and one yeast (*Candida albicans* CIP 444). The minimum inhibitory concentrations (MIC) were determined by serial two-fold dilutions using the conventional broth microdilution method. Inocula were prepared by growing the strains for 24 h in Mueller Hinton (*B. cereus, E. coli* and *P. aeruginosa*), Trypcase-soy (*R. rhodochrous*) or Sabouraud (*C. albicans*) broths. The final inoculum density for the MIC determination was approximately 10^5 organisms mL^{-1}. The microtitre plates were incubated at 27 °C (37 °C for *E. coli*) for 24 to 48 h. The MIC was the lowest concentration of IL inhibiting visible growth of the microorganisms. The MIC determinations were performed in triplicate. The starting concentrations tested depended on the solubility of the ILs in water at 27 °C, which ranged from 95 mM for the most soluble to 2.6 mM for the least soluble ones. All initial concentrations were confirmed by ^{1}H NMR.

Results

Each IL (1 mM) was incubated with *Rhodococcus rhodochrous* ATCC 29672 resting-cells under sterile conditions. A negative control without cells was carried out to monitor potential abiotic degradation of the IL under the same conditions. Samples were taken regularly during a seven-week period and analysed by ^{1}H NMR. Similar experiments were carried out on one example from each category of IL using an activated sludge mixed microbial community supplied by a pharmaceutical wastewater treatment plant (AS) according to the modified OECD protocol (28 d-experiment).[35] All these experiments were carried out in duplicate. The results obtained were very similar (standard deviation: 0-4%; maximum deviation: 7%) and are presented averaging the two independent cultures. For clarity, the results will be presented according to the IL cation.

Biodegradation of pyrrolidinium-based ionic liquids

Neither one of the pyrrolidinium-based ILs studied were degraded under abiotic conditions. However, their biodegradation by *Rhodococcus rhodochrous* was quite rapid within the first 7 d of incubation and then a plateau appeared at 80% and 85% rate of degradation for $[C_1mPyr][Tf_2N]$ and $[C_4mPyr][Tf_2N]$, respectively (Fig. 2). The biodegradation initial rate, considered as first-order kinetics (0-7 d), and the percentage of degradation were very similar for both ILs (Table 1). No metabolite was formed in any significant amount by ^{1}H NMR monitoring during these incubations.

The biodegradation of $[C_4mPyr][Tf_2N]$ by an activated sludge was also tested. No change in IL concentration was observed over the course of the 28 d-incubation period. This cation has already been demonstrated to be recalcitrant to biodegradation by Stolte *et al.* under similar conditions[50] or not "readily biodegradable".[34]

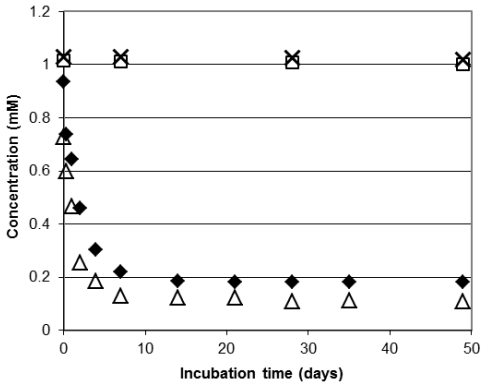

Fig. 2 Degradation kinetics of $[C_1mPyr][Tf_2N]$ (□,◆) and $[C_4mPyr][Tf_2N]$ (**X,** △) under abiotic and biotic conditions with *Rhodococcus rhodochrous* ATCC 29672, respectively. Average of two independent cultures.

Biodegradation of ammonium-based ionic liquids

All of the ammonium-based ILs tested were degraded quite rapidly by *Rhodococcus rhodochrous* but their biodegradation kinetics differed significantly (Table 1). Neither $[N_{1114}][Tf_2N]$, nor $[N_{1132OH}][Tf_2N]$ were degraded under abiotic conditions. Biodegradation by *R. rhodochrous* remained incomplete after 49 d-incubation and 10-20% of the IL was still detected. The presence of a terminal alcohol function did not increase the initial biodegradation rate under the conditions investigated and in the case of $[N_{1132OH}][Tf_2N]$, the percentage of biodegradation was actually lower than for the related alkyl-substituted IL after 49 d-incubation, although they can both be classified as "readily biodegradable" (Fig. 3). However, a direct comparison between these two ILs cannot be made, as the length of the alkyl chains is dissimilar. No significant metabolite was observed in the ^{1}H NMR spectra recorded for either IL.

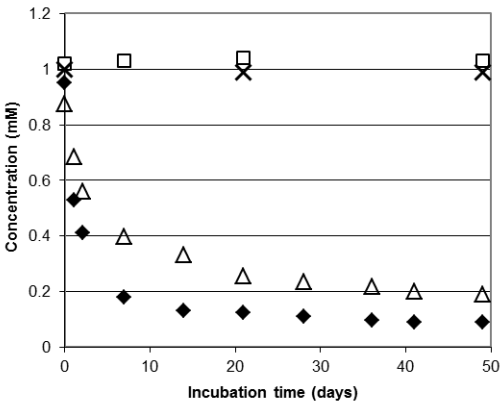

Fig. 3 Degradation kinetics of $[N_{1114}][Tf_2N]$ (□,◆) and $[N_{1132OH}][Tf_2N]$ (**X,** △) under abiotic and biotic conditions with *Rhodococcus rhodochrous* ATCC 29672, respectively. Average of two independent cultures.

Neither was biodegradation observed when $[N_{1132OH}][Tf_2N]$ was incubated with an activated sludge over a period of 28 d.

Table 1 Kinetic parameters of IL degradation under abiotic and biotic (*R. rhodochrous)* conditions

	Abiotic conditions		Biotic conditions			
	Time (d)	% degradation	Time (d)	% degradation	k (d^{-1})	R
$[C_1mPyr][Tf_2N]$	49	0 %	14	80 %	0.20	0.943
$[C_4mPyr][Tf_2N]$	49	0 %	7	85 %	0.24	0.895
$[N_{1114}][Tf_2N]$	49	0 %	28	88 %	0.22	0.938
$[N_{1132OH}][Tf_2N]$	49	0 %	49	79 %	0.10	0.921
$[NH_{112OH}][Ac]$	49	0 %	1	100 %	4.34	0.999
$[N_{1112OOCCH3}][Tf_2N]$	49	24 %	7	100 %	0.73	0.996
$[C_6mPy][Tf_2N]$	49	0 %	49	0%	-	-
$[C_3Py][Tf_2N]$	49	0 %	14	76 %	0.10	0.945
$[C_{3OH}Py][Tf_2N]$	49	0 %	28	85 %	0.081	0.976
$[C_{1COOC2}Py][Tf_2N]$	49	76 %	2	100 %	1.45	0.999

The degradation of $[NH_{112OH}][Ac]$, another ammonium-based ionic liquid containing a terminal alcohol in the cation associated with an acetate anion, proved to be remarkably different. Under abiotic conditions, the ^1H NMR signal for the acetate counteranion (δ = 1.93 ppm; s, -CH_3) disappeared within 30 d of stirring in water (Fig. 4A). This can be explained by a proton transfer reaction with the acetate anion with the subsequent formation of volatile acetic acid.

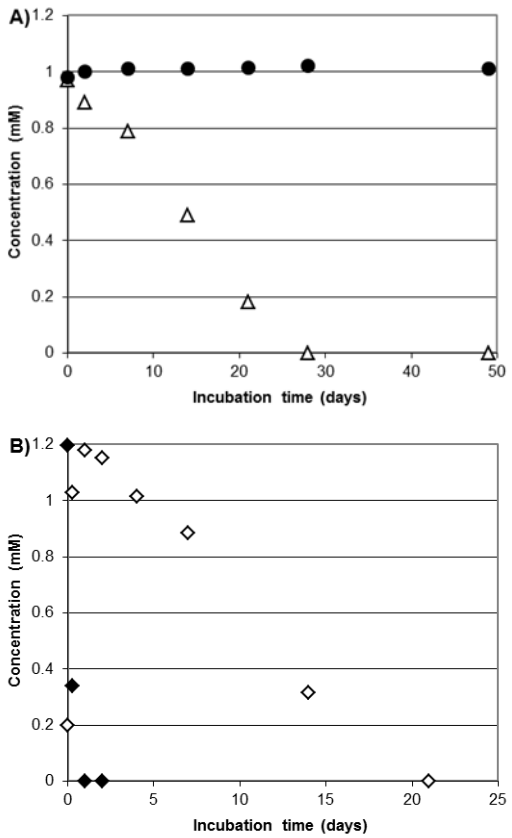

Fig. 4 (**A**) Evolution of the quaternary ammonium cation (●) and acetate anion (△) concentrations measured by ^1H NMR for the species $[NH_{112OH}][Ac]$ under abiotic conditions and (**B**) degradation kinetics under biotic conditions with *Rhodococcus rhodochrous* ATCC 29672: (◆) cation $[NH_{112OH}]$ and (◇) metabolite. Average of two independent cultures.

Conversely, the signals corresponding to the quaternary ammonium cation (δ (D_2O) = 2.90 ppm, s, 6H, -CH_3; 3.23 ppm, t, 2H –N-CH_2, J = 5.3 Hz; 3.90 ppm, 2H, t, -CH_2OH, J = 5.3 Hz) remained unchanged over the entire experiment (Fig. 4A). However, this IL was almost immediately quantitatively biotransformed by *R. rhodochrous* into a new metabolite (δ (D_2O) = 2.93 ppm, s, 6H, -CH_3; 3.73 ppm, s, 2H) (Fig. 4B, Fig. 1, ESI) that was identified as the quaternary ammonium salt of *N*,*N*-dimethylglycine $[N_{111COOH}]$ (Scheme 1) by comparison with literature data.[51] This metabolite then had completely disappeared within 21 d of initial incubation. By contrast, the acetate anion was very rapidly integrated into the central metabolism of the bacterium, and was only evident in the time zero sample.

The final ammonium-based IL studied $[N_{1112OCOCH3}][Tf_2N]$ contained an ester moiety in the long alkyl side chain. The ester function was hydrolyzed even under abiotic conditions (24 % degradation after seven weeks of stirring in water) and the corresponding alcohol-functionalized cation $[N_{1112OH}][Tf_2N]$ accumulated in the medium (δ (D_2O) = 3.20 ppm, s, 9H, -CH_3; 3.52 ppm, t, 2H, J = 5.1Hz, –N-CH_2; 4.04-4.09 ppm, 2H, m, -CH_2OH) (Fig. 5). As previously observed with $[NH_{112OH}][Ac]$, the second hydrolysis product formed (acetate) was only detected in the first samples (T_7-T_{21d}) and had completely disappeared at T_{49d}.

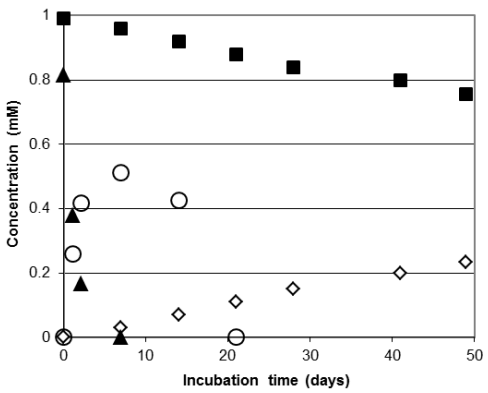

Fig. 5 Degradation kinetics for $[N_{1112OCOCH3}][Tf_2N]$ under abiotic conditions (■) and biotic conditions with *Rhodococcus rhodochrous* ATCC 29672 (▲). Kinetics of formation and degradation for the hydrolysis product under abiotic (◇) and biotic (○) conditions. Average of two independent cultures.

With the bacterium *R. rhodochrous*, the ester, $[N_{1112OCOCH3}][Tf_2N]$ was readily hydrolysed, demonstrating the

importance of biological degradation (Fig. 2, ESI). The alcohol [N_{1112OH}] was the only metabolite detected (Scheme 1). However, this metabolite was in turn biodegraded, and the corresponding ^{1}H NMR integrations decreased after 7 d of incubation to completely disappear after 21 d (Fig. 5).

Biodegradation of pyridinium-based ionic liquids

The long-chain alkylpyridinium IL, [C_6mPy][Tf_2N], resisted degradation under either abiotic or biotic conditions conversely to what was observed (almost fully mineralized (> 97% degradation) after 35-49 d incubation but not considered to be readily biodegradable) with activated sludge microbial communities by Docherty *et al.*[26,38] The microbial diversity, as well as the lower IL concentration used, could explain the different classification of this IL according to the agents and experimental conditions. These contrasted results (not biodegradable versus fully mineralized) emphasize the difficulty in setting up a protocol assessing the biodegradability of ILs in the environment. It is worth noting that under our conditions, the IL concentration in solution increased with time in the presence of microorganisms, reaching nearly the expected initial concentration only after several weeks (Fig. 6). This IL appears to be sorbed rapidly or to interact strongly with cell walls and is then gradually released into the medium. Several new ^{1}H NMR signals appeared during the incubation and may be attributed to compounds released from the bacteria as a result of partial cell wall damage (Fig.3, ESI).[29]

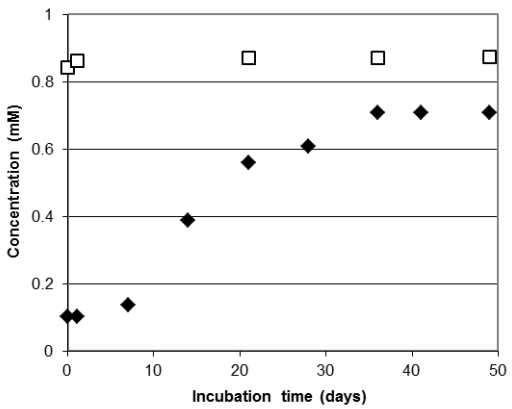

Fig. 6 Degradation kinetics of [C_6mPy][Tf_2N] under abiotic (□) and biotic (◆) conditions with *Rhodococcus rhodochrous* ATCC 29672. Average of two independent cultures.

When the alkyl side chain was shorter (C3, rather than C6), the IL was rendered biodegradable under the test conditions, as opposed to observations by Neumann *et al*. with activated sludge.[34] [C_3Py][Tf_2N] was rapidly biotransformed, to the extent of 76% during the first 14 d of incubation, before a plateau in the biodegradation curve appeared, after which no further biodegradation was observed (Fig. 7A). In this case, only a few compounds released from the bacteria as a result of partial cell wall damage were monitored by ^{1}H NMR.

The introduction of a terminal alcohol into this short alkyl chain had no significant effect on the percentage of biodegradation and the initial rate was actually slower for [C_{3OH}Py][Tf_2N] than [C_3Py][Tf_2N] (Fig. 7B and Table 1).

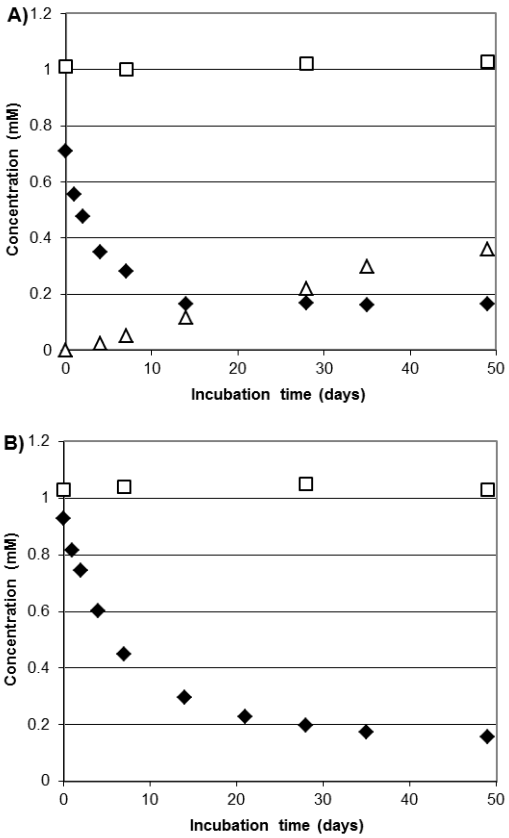

Fig. 7 Degradation kinetics for **A**) [C_3Py][Tf_2N] and **B**) [C_{3OH}Py][Tf_2N] under abiotic (□) and biotic (◆) conditions with *Rhodococcus rhodochrous* ATCC 29672. Evolution of the metabolite (△). Average of two independent cultures.

For both of these ILs, new signals appeared in the ^{1}H NMR spectra over the course of the experiment. In the case of [C_3Py][Tf_2N], each of the signal intensities (spanning a range of chemical shifts) increased equally with time, a result consistent with the formation of a single metabolite: δ (D_2O, ppm) = 0.89 (t, 3H, J = 7.2 Hz); 1.84 (sex, 2H, J = 7.2 Hz); 4.02 (t, 2H, J = 7.2 Hz); 6.60 (d, 2H, J = 7.3 Hz); 7.89 (d, 2H, J = 7.3 Hz) (Fig. 8). The LC-(+)-ESI-MS analyses of various samples taken over the course of the incubation also indicated only one new UV-active peak, which had a shorter retention time (t_R = 3.50 min) than the starting molecule (t_R = 7.85 min). The corresponding MS spectrum indicated an m/z ratio of 138, differing from the molecular weight of [C_3Py] by 16 (Fig. 4, ESI). Thus, the metabolite formed is more polar than the starting molecule and corresponds to a hydroxylated derivative. As only two signals (doublets) are present in the aromatic region, we can conclude that the position of the hydroxyl group induced symmetry in the molecule and is thus in the *para* position of the aromatic ring. Moreover the chemical shifts were compatible with those described for 4-hydroxypyridinium by Wang *et al*.[52] This metabolite was thus identified as the 4-hydroxy-N-propylpyridinium cation [4OH-C_3Py] (Scheme 1). No hydroxylation of the side chain was observed with our bacterial strain contrary to what was determined in previous works with activated sludges.[43-44] This result may be rationalized on the basis that different biodegradation pathways may be accessible, depending upon the microbial strain(s) involved. Hydroxylation of the aromatic ring has already been proposed for similar ILs although the position of the hydroxyl group could not be determined.[38.]It is

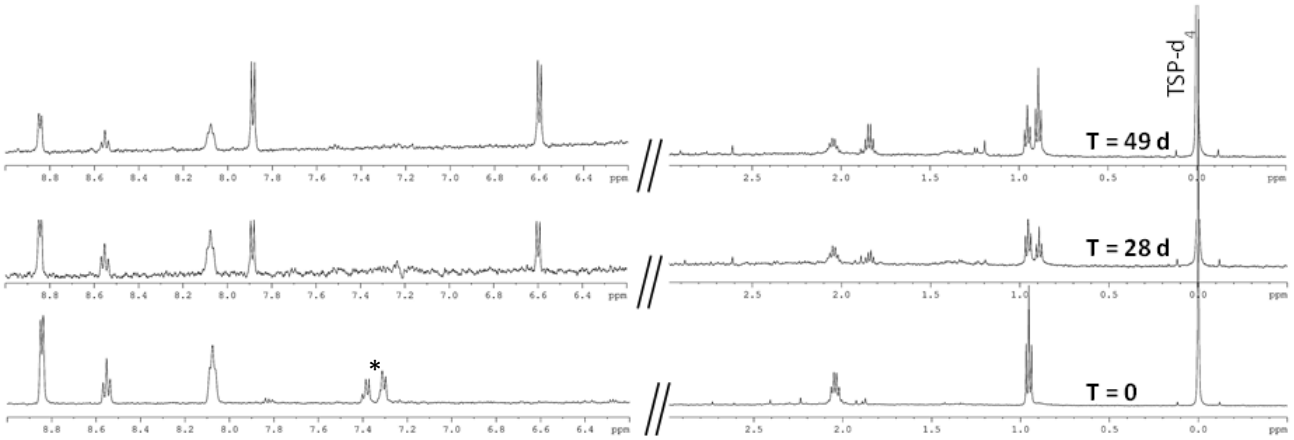

Fig. 8 ^{1}H NMR spectra recorded during the degradation of 1 mM [C_3Py][Tf_2N] by *Rhodococcus rhodochrous* ATCC 29672. (*) Signals present in the cell control.

worth noting that the hydroxylated metabolite is not formed quantitatively, and a delay in its appearance in the supernatant could be due to a lag phase for its excretion as has previously been observed for other metabolites.[53] The concentration of this metabolite increased with time.

In the case of [C_{3OH}Py][Tf_2N], two metabolites were clearly observed, one remaining at a low concentration (the maximum concentration was 50 µM after 21 d of incubation), but disappearing within 35 d (**M1**) and the second one accumulating in the medium (**M2**) (Fig. 9A). According to its ^{1}H NMR spectrum (δ (D_2O, ppm) = 5.81 (d, 2H, J = 7.8 Hz); 7.53 (d, 2H, J = 7.8 Hz)) (Fig. 5, ESI) and its m/z ratio of 96, **M1** could be assigned as the 4-hydroxypyridinium ion. This cation could result from a combination of side chain degradation *via* ω-oxidation and hydroxylation of the aromatic ring, as observed for [C_3Py][Tf_2N]. Metabolite **M1**, remaining at a low concentration in the supernatant, could then be mineralized, probably by enzymatic ring cleavage.

The NMR spectrum of **M2**, which is formed concomitantly with **M1**, exhibits resonances at δ (D_2O) = 2.93 ppm ("t", 2H, J = 6.8 Hz); 7.65 ppm (t, 2H, J = 7.2 Hz); 7.81 ppm (t, 1H, J = 7.8 Hz); 8.35 ppm (d, 2H, J = 6.2 Hz), the three aromatic signals being shifted significantly upfield compared with those of the parent compound (Fig. 5, ESI), and by mass spectrometry (+-ESI) an ion was detected with m/z 152. The HRMS spectrum gave the exact mass of 152.0707 (- 0.5 mDa) corresponding to the formula $C_8H_{10}NO_2$ (+ O – 2H compared with [C_{3OH}Py]) and LC/(+)ESI-MS/MS studies showed fragments at m/z 106, 93, 80 (pyridinium cycle), 78 and 73. Nothing was observed in negative mode. Based on the molecular formula, and ^{1}H NMR data indicating no change in aromatic ring substitution, structures **A**-**F** in Fig. 10 were proposed as **M2**. **A** and **B** were ruled out due to the very labile pyridinium group and would react rapidly with nucleophiles, including water. The tautomers **C** and **D** were inconsistent with the observed peak at 2.93 ppm in the ^{1}H NMR, and thus not considered further. Structure **E** has already been described in the literature[54-55] and cannot explain the shifts observed for the protons in the aromatic region. Structure **F** is consistent with the available data, however concern about the reactivity of the aldehyde group to oxidation and the pyridinium group to nucleophilic substitution (albeit significantly less reactive than **A** and **B**) was noted.

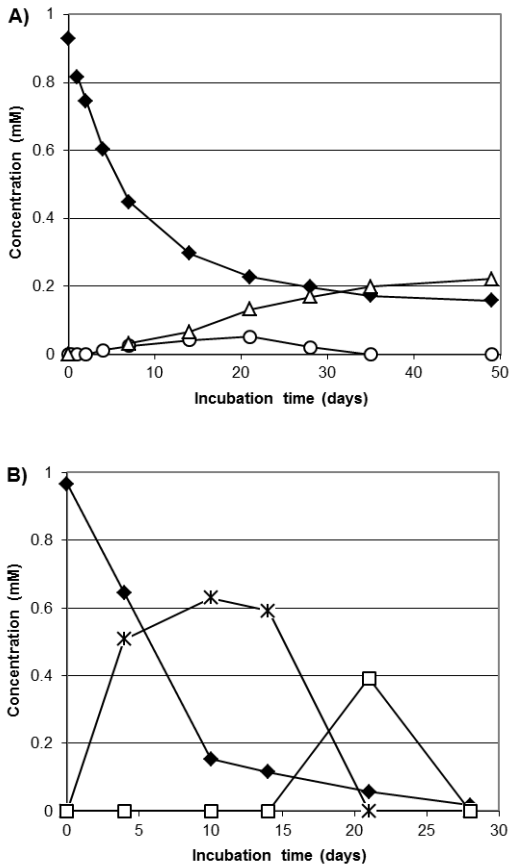

Fig. 9 Biodegradation kinetics of [C_{3OH}Py][Tf_2N] (◆) with (A) *Rhodococcus rhodochrous* ATCC 29672 and (B) activated sludges. Evolution of the four metabolites (○: **M1**; △: **M2**, ✳: **M1s**, □: **M2s**). Average of two independent cultures.

We tentatively propose that there are two possible explanations for the stability of 'beta-hydroxy aldehyde' metabolite **M2**. Firstly, the aldehyde, trimerises to form a 1,3,5-trioxane ring. The beta-hydroxy groups can form stabilising intramolecular hydrogen bonds to the trioxane ring.

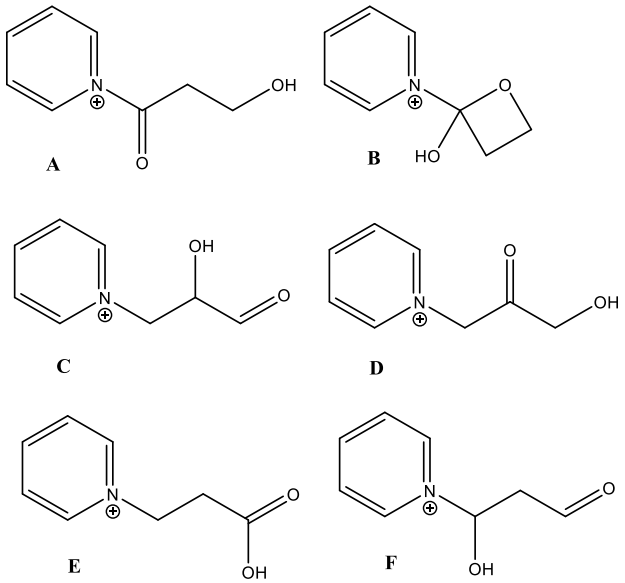

Fig. 10 Possible structures for the metabolite **M2** with a m/z 152.

Figure 11 shows one such structure with hydrogen bonds in 6 membered rings. In water it is envisaged that the trioxane ring can flip between chair conformations. This would account for the absence of a strong geminal coupling at the CH_2, (as now both protons are equivalent) and the coupling then being assigned as a double-doublet. The trioxane ring also is a steric hindrance to approach of nucleophiles, which supports the hypothesis that this class of compounds have lower reactivity than the beta-hydroxy aldehyde. A similar intermediate structure was identified by Pham *et al.*[43] during biodegradation of [C_4mPy] by activated sludge microorganisms using LC-MS. Nevertheless the gamma hydroxyaldehyde formed gives less favorable 7 membered rings on H-bonding to the trioxane ring and this compound was found to decompose rapidly.[43] Secondly, in our case, two molecules of beta-hydroxy aldehyde **E** could form a cyclic diglyceride. However, this would form an 8 membered ring with unfavourable transannular interactions.

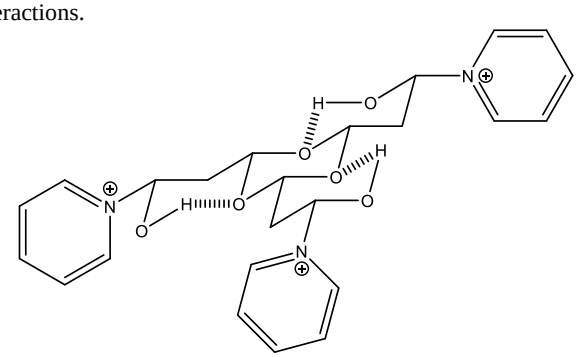

Fig. 11 Proposed structure of **M2** stabilized by intramolecular hydrogen bonds

This IL [C_{3OH}Py][Tf_2N] was also tested using the activated sludge protocol. More than 95% of [C_{3OH}Py][Tf_2N] was degraded within 28 d, at a similar biodegradation rate (k = 0.13 day^{-1}) than the pure strain but with greater efficiently (100% biodegradation) (Fig. 9B). Only two metabolites were clearly observed by ^{1}H NMR, and these were different from those observed using the pure strain, *R. rhodochrous* (Fig. 9B). The first of these metabolites (**M1s**) exhibits a triplet at 2.93 ppm and signals in the aromatic region with similar shifts to those from the parent compound [C_{3OH}Py][Tf_2N] (δ (D_2O): 8.08 ppm (t, 2H, J = 7.5 Hz); 8.56 ppm (t, 1H, J = 7.5 Hz); 8.88 ppm (d, 2H, J = 5.5 Hz)). The second metabolite (**M2s**) was only visible after 21 d of incubation when **M1s** has disappeared and exhibits three aromatic signals at 7.62 (t, 2H, J = 7.5 Hz), 8.01 (t, 1H, J = 7.5 Hz) and 8.62 ppm (d, 2H, J = 7.2 Hz). LC-(+)-ESI-MS analyses gave a m/z ratio of 152 and 110 for **M1s** and **M2s**, respectively. From theoretical and previously reported metabolic pathways for such compounds,[43] the most probable metabolites formed could come from the ω-oxidation of the terminal hydroxyl group to the corresponding acid that is further submitted to β-oxidation. According to the LC-MS and NMR data, **M1s** was assigned as *N*-2-carboxyethylpyridinium ion [C_{2COOH}Py] in agreement with data in the literature[54-55] and **M2s** as *N*-hydroxymethylpyridinium cation [C_{1OH}Py] (Scheme 1). No other metabolites were detected over the course of the experiment and it is possible that complete mineralization of the IL occurred in the presence of the microbial community.

The effect of an ester functional group in the alkyl side chain was also tested, using [C_{1COOC2}Py][Tf_2N]. As was observed with [$N_{1112OCOCH3}$][Tf_2N] (*vide supra*), the ester was readily hydrolyzed under both abiotic and biotic conditions. The formation of hydrolysis products ([C_{1COOH}Py] and ethanol) was monitored by ^{1}H NMR under abiotic conditions, with 76% hydrolysis occurring after 49 d stirring in water (Fig. 12). The carboxylic acid derivative was identified by ^{1}H NMR (δ (D_2O, ppm) = 5.23 (s, 2H); 8.09 (t, 2H, J = 7.0 Hz); 8.58 (t, 1H, J = 7.9 Hz); 8.76 ppm (d, 2H, J = 6.8 Hz)) and LC-MS: retention time 8.9 min; m/z = 138 (both NMR and LC-MS data agreed with the literature) (Fig. 6, ESI).[55-56] The same ester hydrolysis occurred immediately in the presence of *R. rhodochrous*, giving the corresponding acid [C_{1COOH}Py], (Scheme 1) which accumulated in the medium, in quantitative yield (Fig. 12). Ethanol was not detected in these samples and was therefore very rapidly integrated into the central metabolism of the bacterium.

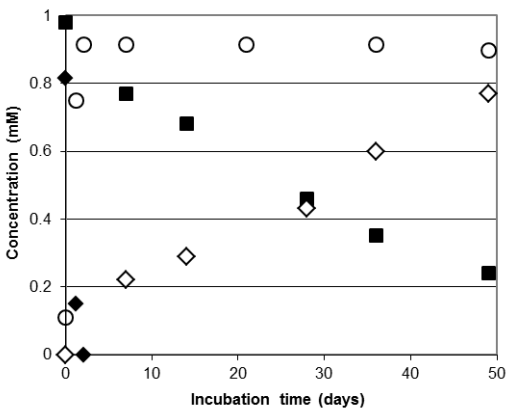

Fig. 12 Degradation kinetics of [C_{1COOC2}Py][Tf_2N] under abiotic (■) and biotic (◆) conditions with *Rhodococcus rhodochrous* ATCC 29672. Appearance of the hydrolysis product under abiotic (◇) and biotic (○) conditions. Average of two independent cultures.

Biodegradation of the counteranion

As has been previously discussed, the acetate counteranion was rapidly integrated into the central metabolism of *Rhodococcus rhodochrous* (Fig. 4A). Experiments were also carried out to monitor the fate of the bis(trifluoromethylsulfonyl)imide counteranion. ^{19}F NMR spectra of samples taken at 0 and 49 d were recorded on one IL in each series. No change in the intensity of the [Tf_2N] peak and

Table 2 Minimum Inhibitory Concentrations (MIC) of ionic liquids (mM) to Gram positive and negative bacteria and a yeast strain. *B.c. Bacillus cereus* ATCC 14579*; P.a. Pseudomonas aeruginosa* ATCC 17504*; E.c. Escherichia coli* ATCC 11303*; R.r. Rhodococcus rhodochrous* ATCC 29672*; C.a. Candida albicans* CIP 444

	B.c. (+)	*P.a.* (-)	*E.c.* (-)	*R.r.* (+)	*C.a.*
$[C_1mPyr][Tf_2N]$	> 12	> 12	12	> 12	> 12
$[C_4mPyr][Tf_2N]$	> 2	> 2	> 2	> 2	> 2
$[N_{1114}][Tf_2N]$	> 12.5	> 12.5	6.3	> 12.5	> 12 5
$[N_{1132OH}][Tf_2N]$	45	> 45	22.5	45	> 45
$[NH_{112OH}][Ac]$	> 47.5	> 47.5	> 47.5	47.5	> 47.5
$[N_{1112OOCCH3}][Tf_2N]$	> 30	> 30	15	> 30	> 30
$[C_6mPy][Tf_2N]$	1.3	> 1.3	0.3	0.6	> 1.3
$[C_3Py][Tf_2N]$	15	>15	3.8	15	> 15
$[C_{3OH}Py][Tf_2N]$	> 15	> 15	15	> 15	> 15
$[C_{1COOC2}Py][Tf_2N]$	15	> 15	15	15	> 15

no appearance of new signals were monitored. This anion was therefore not biodegraded by our bacterial strain. The same conclusions were obtained with the activated sludges. This type of fluorinated anion has been shown to be among the most recalcitrant to biodegradation under aerobic and anaerobic conditions.[57]

Anti-microbial activities and toxicities

1 Agar diffusion test. The adapted Agar diffusion method[58-60] was first tested as an easy-to-implement qualitative evaluation of the anti-microbial activities of the ILs studied toward two Gram-negative bacterial strains (*Escherichia coli* DSMZ 498 and *Pseudomonas putida* CP1). Aqueous solutions of IL at 2g L^{-1} were first tested and showed no inhibition towards either species of bacteria.

2 Determination of Minimum Inhibitory Concentrations (MIC). Five strains were tested to assess the antimicrobial activity of the ILs: four bacteria (*Bacillus cereus* ATCC 14579 and *Rhodococcus rhodochrous* ATCC 29672 as Gram positive bacteria, *Pseudomonas aeruginosa* ATCC 17504 and *Escherichia coli* ATCC 11303 as Gram negative bacteria) and one yeast (*Candida albicans* CIP 444). The ILs tested encompass a wide range of solubilities in water. In order to avoid the complication of including additional solvents to dissolve the IL, or possible problems from IL precipitation in the medium after solvent evaporation, the choice was made to adapt the starting IL concentration for MIC evaluation to correspond with its solubility. The initial IL concentration was confirmed by NMR. The minimum inhibitory concentrations (MIC values) for the ILs are listed in Table 2.

One has to exercise caution comparing the MIC results of chemicals when experiments are carried out at different concentrations depending on their aqueous solubility, as bioavailability becomes an important addition consideration. The solubility of the ILs in the test medium ranged from 2.6 mM for $[C_6mPy][Tf_2N]$ to 95 mM for $[NH_{112OH}][Ac]$. Nevertheless, the experimental procedure requires the dilution of the highest concentration by two due to addition of the microbial suspension. Only one IL $[C_4mPyr][Tf_2N]$ has MIC values, for all 5 microbial strains, above the solubility, albeit 2 mM. However, to state that this is the least toxic of the ILs in this study could be potentially misleading. $[NH_{112OH}][Ac]$ has a MIC value of 47.5 mM for *Rhodococcus rhodochrous* and > 47.5 mM (solubility) for the remaining microbial strains in the test. Nevertheless, despite this issue of comparing MIC values, we have determined that most of the ILs studied do not present any acute toxicity towards the microorganisms screened, as their MIC is near their solubilities, except in the case of the long chain alkyl IL $[C_6mPy]$. The strain *E. coli* has been found to be the more sensitive to the ILs tested as previously observed.[29]

Discussion

Nine of the ten pyrrolidinium, pyridinium and ammonium ILs tested (1 mM) were biodegraded by *Rhodococcus rhodochrous* ATCC 29672 with a biodegradation percentage > 75% within 28 d. The only exception was $[C_6mPy][Tf_2N]$, which has already been shown to slowly biodegrade[30] or even be recalcitrant[50] depending on the microbial community used.[38] This compound was also found to be the most toxic towards microbial cells.[this study,29,61] With the activated sludge, only one of the tested ILs, $[C_{3OH}Py][Tf_2N]$ was degraded. These results demonstrate that the origin and adaptation of a microbial community, the culture conditions,[30,39] and of course the microorganism(s) present can lead to completely different conclusions on the biodegradability of chemicals.

The kinetics of biodegradation by *R. rhodochrous* for this series of ILs were also very different (Table 1). Rates of biodegradation were found to vary by up to a factor of 50 in the case of $[NH_{112OH}][Ac]$ compared to more recalcitrant pyridinium derivatives, even containing a hydroxyl group $[C_{3OH}Py][Tf_2N]$. It is worth emphasizing that the use of a resting-cell bacterium could explain the plateau observed in all the cases for which kinetics experiments were incomplete after 20-40 d of biodegradation. In general, the pyridinium-based ILs were more slowly degraded, although introduction of an ester group into the side chain increased both the rate and the extent of the biodegradation.[62] It is worth noting that the hydrolysis reaction occurred also under our abiotic conditions in a significant proportion (in particular for $[C_{1COOC2}Py]$ with 55% after 28 d making this compound difficult to use with water in the long-term). Notably, the same effect was not observed

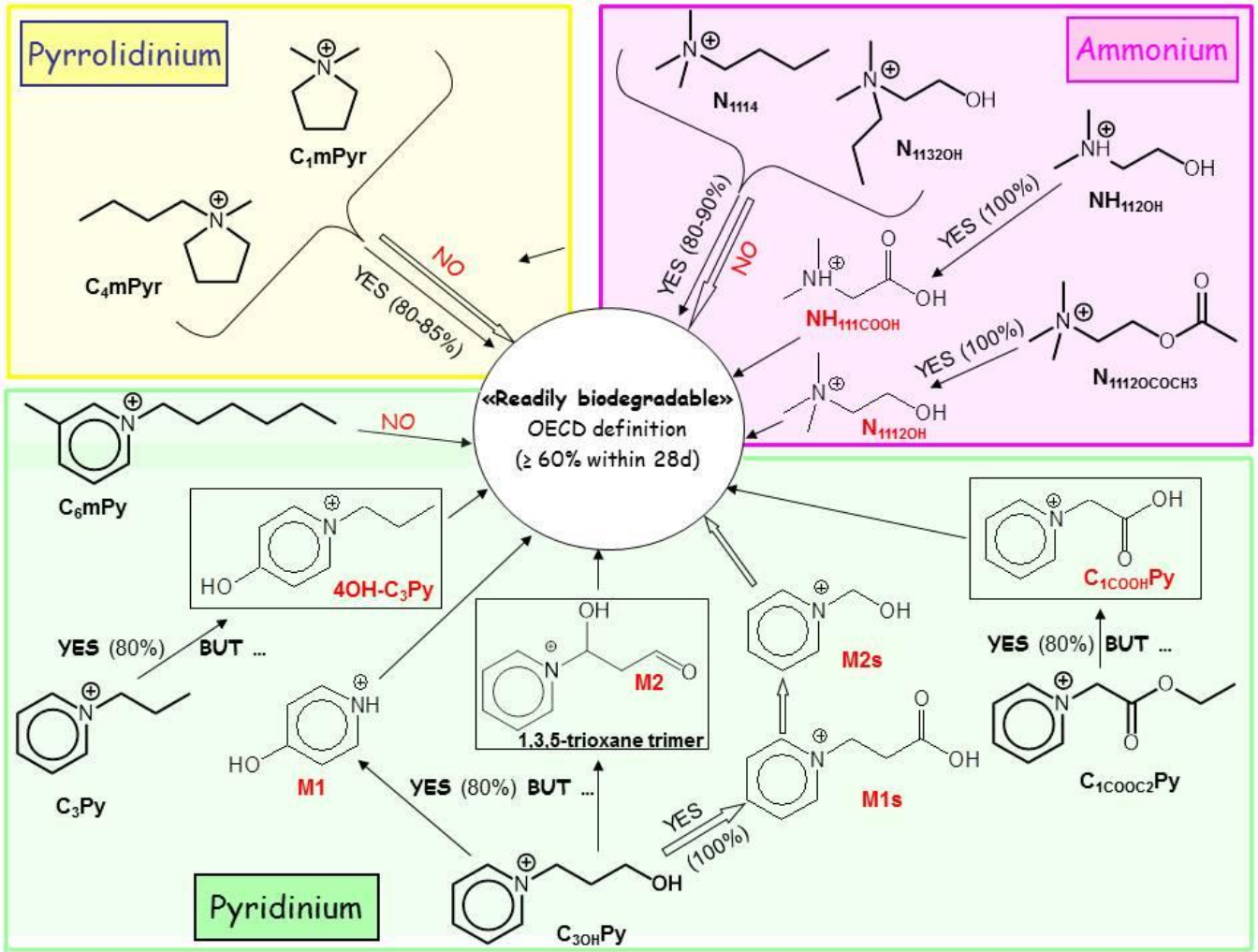

Scheme 1 Proposed biodegradation pathways of pyrrolidinium, ammonium and pyridinium-based ILs by *Rhodococcus rhodochrous* ATCC 29672 (→) and activated sludges (⇨). The degradation percentage for the **parent molecule** is indicated in brackets. The metabolites in boxes accumulate in the medium.

when a terminal hydroxyl group was incorporated. Indeed the introduction of a terminal hydroxyl moiety did not boost the degradation rate and even decreased it in the case of [C_{3OH}Py].

Ammonium-based ILs were more rapidly degraded, if not completely substituted with long alkyl chains, especially when the counter anion was acetate. Interestingly, for pyrrolidinium ILs and our bacterial pure strain, the rate of biodegradation was not significantly affected by the length of the *N*-alkyl side chain (in the range between C1 and C4) as opposed to what was described in the literature with activated sludges.[30]

In accordance with previous reports in the literature,[20-21,40,63-64] the most toxic IL is the one with the longest alkyl side chain: [C_6mPy][Tf_2N] and the introduction of oxygen-functionalization greatly reduced the toxicity.[23-25,28-29] Our results confirm the relationship between IL hydrophobicity and toxicity already described for other organisms[20,63-65] Differences were also observed between the microbial strains tested, with *Escherichia coli* proving the most sensitive towards IL toxicity, while *Pseudomonas aeruginosa* and *Candida albicans* were most resistant.

Whilst almost all these ILs were found to be "readily biodegradable" in the presence of *R. rhodochrous*, it is also important to know which metabolites are formed and whether these are only intermediate or can accumulate in the medium. To the best of our knowledge, this is the first study to describe detailed, unambiguous biodegradation pathways for ILs, determined using complementary techniques (NMR / MS) to confidently assign IL metabolites (Scheme 1).

In summary (Scheme 1), the pyrrolidinium- and ammonium-based ILs tested were considered to be "readily biodegradable" only with the pure strain *Rhodococcus rhodochrous* ATCC 29672 used in resting-cell conditions, the biodegradation rate being > 80% within 28 d of incubation. Some intermediate metabolites were identified in the case of [NH_{112OH}][Ac] and [$N_{1112OCOCH3}$][Tf_2N] corresponding to ω-oxidation and hydrolysis transformation reactions, respectively. They were then biotransformed in their turn. The introduction of a terminal hydroxyl group on the alkyl chain did not enhance the biodegradation rate. The nature of the counteranion is also important as the [Ac] was readily incorporated in the central metabolism of the bacterium whereas [Tf_2N] was not biodegraded. Conversely, no biodegradation occurred with the activated sludges chosen.

For the pyridinium-based ILs, the results were more contrasted with *R. rhodochrous*: the long alkyl chain [C_6mPy][Tf_2N] was not degraded and seems to lead to cell wall damage and / or adsorption;[14,43,66-68] all the other ILs tested from this family were classified as "readily biodegradable" as the parent IL was degraded more than 80% within 28 d of incubation but metabolites resulting from hydroxylation on the alkyl chain or aromatic ring or hydrolysis of the terminal ester moiety accumulated in the medium. These metabolites could present different environmental behaviours and toxic activities from the starting ILs and could therefore impact ecosystems. By comparing the [C_{3OH}Py][Tf_2N] biodegradation with the pure bacterial strain *R. rhodochrous* and activated sludges, different pathways were established due to the presence of distinct microorganisms, showing the numerous potential more or less reactive metabolites that can be generated in the environment. Nevertheless this IL was found to be "readily biodegradable" in both cases, emphasizing the difficulty assessing the environmental behaviour of ILs.

Conclusions

In this investigation, we have demonstrated that not only "classical" biodegradation pathways, such as ω-oxidation, are operating in the microbial breakdown of ILs. More surprisingly, *p*-hydroxylation of the pyridinium ring (already suggested by Docherty *et al*.[38]) or cyclization reaction after oxidation of the alkyl chain, as well as more conventional ester hydrolysis occurred. These mechanisms lead to reactive metabolites that accumulate in the medium and can impact the environment although the parent IL has been shown to be "readily biodegradable". Distinct pathways have also been observed for the same IL, [C_{3OH}Py][Tf_2N] from the action of different microorganisms, demonstrating the diversity of potential metabolites which may be formed in the environment. Clearly, the toxicity and biodegradability of these metabolites must be thoroughly accounted for in any assessment of the environmental impact of ILs. Our work draws attention to the limitations, even 'flaws' of the readily biodegradation tests and the requirement for further studies. It emphasizes also the need to better characterize the sludges from wastewater treatment plant used and to standardize the culture conditions to have a "normalized" test. However, crucially it is important to understand what is a 'readily biodegradation' test. It is not a bioaccumulation assay or an ultimate biodegradation (mineralization) test, and the results for readily biodegradation tests must be considered mindful of the limitations (for example formation of some persistent metabolites) of the test. Moreover it is primordial to take into account the ILs metabolites and their potential impact on environment for their global life cycle risk assessment. Furthermore, it is required to determine the structure and identify the various metabolites potentially formed in the environment from the diverse ILs in use in order to assess their toxicity and environmental behaviour in detail.

Acknowledgements

The authors greatly acknowledge A. Abila and A.-S. Biesse-Martin for the MS and 2D-NMR analyses of some IL metabolites, respectively. This work has been financially supported by the France/Ireland bilateral collaboration project Ulysses. Y.D. has been financed by the project CPER Environment of the Auvergne Region, France.

Notes and References

[a] Clermont Université, Université Blaise Pascal, Institut de Chimie de Clermont-Ferrand, BP 10448, F-63000 Clermont-Ferrand, France.
[b] CNRS, UMR 6296, ICCF, BP 80026, F-63171 Aubière, France
[c] School of Chemical Sciences, Dublin City University, Glasnevin, Dublin 9, Ireland.
[d] National Institute of Cellular Biology, Dublin City University, Glasnevin, Dublin 9, Ireland.
[e] School of Biotechnology, Dublin City University, Dublin 9, Ireland.

1 J.H. Davis, *Chem. Lett.,* 2004, **33,** 1072-1077.
2 R. Giernoth, *Angew. Chem. Int. Ed*., 2010, **49**, 5608-5609.
3 M. Petkovic, K. R. Seddon, L. P. N. Rebelo and C. Silva, *Chem. Soc. Rev*., 2011, **40,** 1383-1403.
4 E. A. Khokhlova, V. V. Kachala and V. P. Ananikov, *ChemSusChem,* 2012, **5**, 783-789.
5 N. V. Plechkova and K. R. Seddon, *Chem. Soc. Rev.*, 2008, **37**, 123-150.
6 S. Tang, G. A. Baker and H. Zhao, *Chem. Soc. Rev.*, 2012, **41**, 4030-4066.
7 A. S. Wells and V. T. Coombe, *Org. Process Res. Dev.*, 2006, **10**, 794–798.
8 C. W. Cho, T. P. T Pham, Y. C. Jeon, K. Vijayaraghavan, W. S. Choe and Y. S. Yun, *Chemosphere*, 2007, **69**, 1003-1007.
9 K. J. Kulacki and G. A. Lamberti, *Green Chem.*, 2008, **10**, 104-110.
10 M. M. Bailey, M. B. Townsend, P. L. Jernigan, J. Sturdivant, W. L. Hough-Troutman, J. F. Rasco, R. P. Swatloski, R. D. Rogers and R. D. Hood, *Green Chem*., 2008, **10,** 1213-1217.
11 Y. Cheng, S. H. Wright, M. J. Hooth and I. G. Sipes, *Drug Metab. Dispos*., 2009, **37**, 909-916.
12 A. Latala, M. Nedzi and P. Stepnowski, *Green Chem.*, 2009, **11**, 580-588.
13 C. Pretti, C. Chiappe, I. Baldetti, S. Brunini, G. Monni and L. Intorre, *Ecotox. Environ. Safe*., 2009, **72**, 1170-1176.
14 T. P. T. Pham, C.-W. Cho and Y.-S. Yun, *Water Res*., 2010, **44**, 352-372.
15 S. Steudte, P. Stepnowski, C.-W. Cho, J. Thöming and S. Stolte, *Chem. Commun*., 2012, **48**, 9382-9384.
16 K.S. Egorova and V.P. Ananikov, *ChemSusChem*, 2014, **7**, 336-360.
17 J. S. Torrecilla, J. Palomar, J. Lemus and F. Rodríguez, *Green Chem*., 2010, **12**, 123-134.
18 M. Alvarez-Guerra and A. Irabiena, *Green Chem*., 2011, **13**, 1507.1516.
19 F. Yan, S. Xia, Q. Wang and P. Ma, *J. Chem. Eng. Data*, 2012, **57**, 2252-2257.
20 P. Izadiyan,M. H. Fatemi and M. Izadiyan, *Ecotox. Environ. Safe*., 2013, **87**, 42-48.
21 D. Coleman, M Špulák, M. T. Garcia and N. Gathergood, *Green Chem*., 2012, **14**, 1350-1356.
22 R. Ferraz, V. Teixeira, D. Rodrigues, R. Fernandes, C. Prudêncio, J.P. Noronha, Z. Petrovski and L. C. Branco, *RSC Adv.*, 2014, 4301-4307.
23 N. Gathergood, M. T. Garcia and P. J. Scammells, *Green Chem*., 2004, **6**, 166-175.
24 M. T. Garcia, N. Gathergood and P. J. Scammells, *Green Chem.*, 2005, **7**, 9-14.

25 N. Gathergood, P. J. Scammells and M. T. Garcia, *Green Chem.*, 2006, **8,** 156-160.
26 K. M. Docherty, J. K. Dixon and C. F. Kulpa Jr, *Biodegradation*, 2007, **18**, 481-493.
27 J. R. Harjani, R. D. Singer, M. T. Garcia and P. J. Scammells, *Green Chem*., 2009, **11**, 83-90.
28 S. Morrissey, B. Pegot, D. Coleman, M. T. Garcia, D. Ferguson, B. Quilty and N. Gathergood, *Green Chem*., 2009, **11**, 475-483.
29 Y. Deng, P. Besse-Hoggan, M. Sancelme, A-M. Delort, P. Husson and M.F. Costa Gomes, *J. Hazard. Mater.*, 2011, **198**, 165-174.
30 N. Ferlin, M. Courty, S. Gatard, M. Spulak, B. Quilty, I. Beadham, M. Ghavre, A. Haiß, K. Kümmerer, N. Gathergood and S. Bouquillon, *Tetrahedron*, 2013, **69**, 6150-6161.
31 L. Myles, R. G. Gore, N. Gathergood and S. J. Connon, *Green Chem*., 2013, **15**, 2740-2746.
32 R. G. Gore, L. Myles, M. Spulak, I Beadham, T. M. Garcia, S. J. Connon and N. Gathergood, *Green Chem*., 2013, **15**, 2747-2760.
33 S. P. M. Ventura, M. Gurbisz, M. Ghavre, F. M. M. Ferreira, F. Gonçalves, I. Beadham, B. Quilty, J. A. P. Coutinho and N. Gathergood, *ACS Sustainable Chem. Eng.*, 2013, **1**, 393-402.
34 J. Neumann, S. Steudte, C.-W. Cho, J. Thöming and S. Stolte, *Green Chem*., 2014, **16**, 2174-2184.
35 OECD Guidelines for Testing of Chemicals: ready biodegradability, 301, Paris, France, 1992.
36 D. Coleman and N. Gathergood, *Chem. Soc. Rev.*, 2010**,** **39**, 600-637.
37 I. Beadham, M. Gurbisz and N. Gathergood, 2012, Handbook of Green Chemistry, Chapter 6, Volume 9: Designing Safer Chemicals, First Edition. Edited by Robert Boethling and Adelina Voutchkova, Wiley-VCH Verlag GmbH & Co. KGaA, pp 137-158.
38 K. M. Docherty, M. V. Joyce, K. J. Kulacki and C. E. Kulpa, *Green Chem*., **2010**, *12*, 701-712.
39 M. Markiewicz, S. Stolte, Z. Lustig, J. Luczak, M. Skup, J. Hupka and C. Jungnickel, *J. Hazard Mater.*, 2011, **195**, 378-382.
40 M. Markiewicz, M. Piszora, N. Caicedo, C. Jungnickel and S. Stolte, *Water Res*., 2013, **47**, 2921-2928.
41 S. Kumar, W. Ruth, B. Sprenger and U. Kragl, *Chem. Today*, 2006, **24**, 70-72.
42 S. Stolte, S. Abdulkarim, J. Arning, A.-K. Blomeyer-Nienstedt, U. Bottin-Weber, M. Matzke, J. Ranke, B. Jastorff and J. Thöming, *Green Chem*., 2008, **10,** 214-224.
43 T. P. T. Pham, C.-W. Cho, C.-O. Jeon, Y.-J. Chung, M. W. Lee and Y.-S. Yun, *Environ. Sci. Technol.,* 2009, **43**, 516-521.
44 T. P. T. Pham, C.-W. Cho and Y.-S. Yun, *Water Res*., 2010, **44**, 352-372.
45 J. Neumann, O. Grundmann, J. Thöming, M. Schulte and S. Stolte, *Green Chem*., 2010, **12**, 620-627.
46 C. Zhang, S.V. Malhotra and A.J. Francis, *Chemosphere,* 2011, **82**, 1690-1695.
47 S. Stolte, S. Steudte, A. Igartua and P. Stepnowski, *Curr. Org. Chem*., 2011, **15,** 1946-1973.
48 U. Domanska, E. Bogel-Lukasik and R. Bogel-Lukasik, *Chem. Eur. J.*, 2003, **9**, 3033-3041.
49 A. Chapeaux, L. D. Simoni, M. A. Stadtherr and J. F. Brennecke, *J. Chem. Eng. Data*, 2007, **52**, 2462-2467.
50 S. Stolte, S. Steudte, O. Areitioaurtena, F. Pagano, J. Thöming, P. Stepnowski and A. Igartua, *Chemosphere*, 2012, **9**, 1135-1141.
51 M. J. Simpson and J. R. McKelvie, *Anal. Bioanal. Chem*., 2009, **394**, 137-149.
52 Y. J. Wang, K. Chen and L. M. Tang, *Chem. Letter*, 2009**,** **38**, 472-473.
53 L. El-Bassi, H. Iwasaki, H. Oku, N. Shinzato and T. Matsui, *Chemosphere*, 2010, **81**, 109-113.
54 M. Szafran, Z. Dega-Szafran, B. Nowak-Wydra and M. Piertrzak, *J. Mol. Struc*., 2001, **563-564**, 555-564.
55 T. Thorsteinsson, M. Másson, K. G. Kristinsson, M. A. Hjálmarsdóttir, H. Hilmarsson and T. Loftsson, *J. Med. Chem*., 2003, **46**, 4173-4181.
56 X.-M. Chen and T. C. W. Mak, *J. Chem. Soc., Dalton Trans.*, 1992, 1585-1590.
57 J. Neumann, C.-W. Cho, S. Steudte, J. Köser, M. Uerdingen, J. Thöming and S. Stolte, *Green Chem.*, 2012, **14**, 410-418.
58 M. Rebros, H. Q. N. Gunaratne, J. Ferguson, K. R. Seddon and G. Stephens, *Green Chem*., 2009, **11**, 402–408.
59 N Wood and G. Stephens, *Phys. Chem. Chem. Phys.*, 2010, **12**, 1670-1674.
60 S. P. M. Ventura, R. L. F. de Barros, T. Sintra, C. M. F. Soares, A. S. Lima and J. A. P. Coutinho, *Ecotoxicol. Environ. Saf.*, 2012, **83,** 55-62.
61 G. Quijano, A. Couvert, A. Amrane, G. Darracq, C. Couriol, P. Le Cloirec, L. Paquin and D. Carrié, *Chem. Eng. J.*, 2011, **174**, 27-32.
62 L. Ford, J. R. Harjani, F. Atefi, M. T. Garcia, R. D. Singer and P. J. Scammells, *Green Chem.*, 2011, **12**, 1783-1789.
63 D. J. Couling, R .J. Bernot, K. M. Docherty, J. K. Dixon and E .J. Maginn, *Green Chem*., 2006, **8**, 82-90.
64 A. Romero, A. Santos, J. Tojo and A. Rodriguez, *J. Haz. Mater*., 2008, **151**, 268-273.
65 S. Viboud, N. Papaiconomou, A. Cortesi, G. Chatel, M. Draye and D. Fontvieille, *J. Haz. Mater.*, 2012, **215-216**, 40-48.
66 K. M. Docherty and C. F. Kulpa, Jr *Green Chem.*, 2005, **7**, 185-189.
67 J. I. Khudyakov, P. D'Haeseleer, S. E. Borglin, K. M. De Angelis, H. Woo, E. A. Linquist, T. C. Hazen, B. A. Simmons and M. P. Thelen, *Proc. Natl. Acad. Sci. U.S.A*. 2012, **109**, 2173-2182.
68 M. Zakrewsky, K. S. Lovejoy, T. L. Kern, T. E. Miller, V. Le, A. Nagy, A. M. Goumas, R. S. Iyer, R. E. Del Sesto, A. T. Koppisch, D. T. Fox and S. Mitragotri *Proc. Natl. Acad. Sci. U.S.A.* 2014, **111,** 13313-13318.

When can ionic liquids be considered readily biodegradable? Biodegradation pathways of pyridinium, pyrrolidinium and ammonium-based ionic liquids

Yun Deng, Ian Beadham, Mukund Ghavre, Margarida F. Costa Gomes, Nicholas Gathergood, Pascale Husson, Bertrand Légeret, Brid Quilty, Martine Sancelme and Pascale Besse-Hoggan

The biodegradation pathways of different class ionic liquids by *Rhodococcus rhodochrous* ATCC29672 and an activated sludge showed metabolite accumulation.